Computer methods in applied mechanics and engineering

Comput. Methods Appl. Mech. Engrg. 120 (1995) 389–402

Design of laminated composite plates for optimal dynamic characteristics using a constrained global optimization technique

T.Y. Kam*, F.M. Lai

Department of Mechanical Engineering, National Chiao Tung University, Hsin-Chu 30050, Taiwan, ROC

Received 22 November 1993

Abstract

The lamination arrangements of moderately thick laminated composite plates for optimal dynamic characteristics are studied via a constrained multi-start global optimization technique. In the optimization process, the dynamical analysis of laminated composite plates is accomplished by utilizing a shear deformable laminated composite finite element, in which the exact expressions for determining shear correction factors were adopted, and the modal damping model constructed based on an energy concept. The optimal layups of laminated composite plates with maximum fundamental frequency or modal damping are then designed by maximizing the frequency or modal damping capacity of the plate via the multi-start global optimization technique. The effects of length-to-thickness ratio, aspect ratio and number of layer groups upon the optimum fiber orientations or layer group thicknesses are investigated by means of a number of examples of the design of symmetrically laminated composite plates.

1. Introduction

Because of their light weight and many superior properties, laminated composite plates or panels have been widely used in the construction of vehicle, aircraft and spacecraft structures. In general, these structures are subjected to dynamical loadings and, if the structures are not properly designed, they may fail due to dynamical instability or fatigue. Therefore, the study of dynamic behavior of fiber-reinforced composite plates has attracted close attention in recent years. In particular, since damping has the beneficial effects on stabilizing vibration and elongating fatigue life of structures, the studies of damping capacities of laminated composite structures have been carried out by many investigators [1–8]. For instance, Adams and his associates [1–3] studied the modal damping capacity of laminated composite beams and plates based on an energy concept. Alam and Asnani [4] investigated the modal damping of laminated composite plates via the complex modulus approach. It is noted that the results obtained by the previous researchers were only available for thin laminated composite plates (length-to-thickness ratio was about 150). To take advantage of the flexibility of laminated composite materials in tailoring, it is worth investigating the optimal layups that can make laminated composite structures possess the best dynamic characteristics. Recently, Kam and his associates [9–12] used an unconstrained global optimization technique to investigate the optimal fiber angles for enhancing the mechanical performance of laminated composite plates. Since ply group thicknesses have important effects on the dynamic behavior of laminated composite structures, in addition to fiber angles it is worth including ply group thicknesses in the optimal design of laminated composite structures for better dynamic performance. As is well known, the transverse shear deformation may have significant effects

* Corresponding author.

0045-7825/95/$09.50 © 1995 Elsevier Science S.A. All rights reserved
SSDI 0045-7825(94)00063-S

on the behavior of moderately thick laminated composite plates due to the thickness effect and the low transverse shear modulus relative to the in-plane Young's moduli. It is, therefore, worth studying how the transverse shear deformation as well as the other factors such as aspect ratio, length-to-thickness ratio and number of layer groups affect the lamination arrangement for optimal dynamic characteristics of moderately thick laminated composite plates.

This paper uses a previously proposed shear deformable finite element [13] and the modal damping model established based on an energy concept to study the dynamic characteristics of moderately thick laminated composite plates. The optimal layups for the plates with maximum fundamental frequency or modal damping are determined by maximizing, respectively, the frequency or modal damping capacity of the plates via a constrained multi-start global optimization technique. The effects of length-to-thickness ratio, aspect ratio and number of layer groups upon the optimum lamination arrangements and the values of frequency or damping of the plates are investigated by means of a number of examples.

2. Vibration of laminated composite plate

Consider a rectangular plate of area $a \times b$ and constant thickness h subject to dynamic forces as shown in Fig. 1. The plate is composed of a finite number of layer groups in which each layer group contains several orthotropic layers of same fiber angle and uniform thickness. The x and y coordinates of the plate are taken in the midplane of the plate. The displacement field is assumed to be of the form

$$\begin{aligned} u_1(x, y, z, t) &= u_0(x, y, t) + z \cdot \psi_x(x, y, t) \\ u_2(x, y, z, t) &= v_0(x, y, t) + z \cdot \psi_y(x, y, t) \\ u_3(x, y, z, t) &= w(x, y, t) \end{aligned} \tag{1}$$

where t is time; u_1, u_2, u_3 are displacements in the x, y, z directions, respectively, and u_0, v_0, w the associated midplane displacements; and ψ_x and ψ_y are shear rotations.

The plate constitutive equations are written as

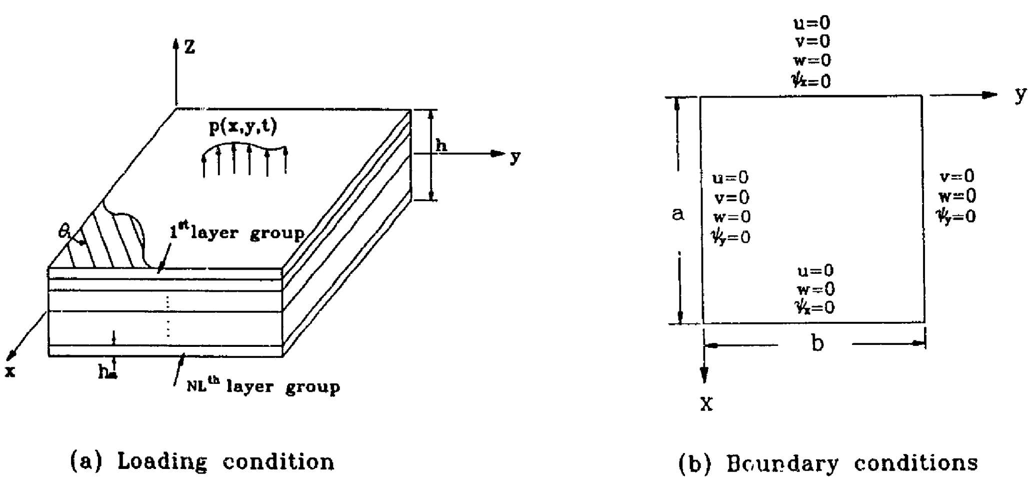

Fig. 1. Laminated composite plate.

$$\begin{bmatrix} N_1 \\ N_2 \\ Q_y \\ Q_x \\ N_6 \\ M_1 \\ M_2 \\ M_6 \end{bmatrix} = \begin{bmatrix} A_{11} & A_{12} & 0 & 0 & A_{16} & B_{11} & B_{12} & B_{16} \\ A_{12} & A_{22} & 0 & 0 & A_{26} & B_{12} & B_{22} & B_{26} \\ 0 & 0 & A_{44} & A_{45} & 0 & 0 & 0 & 0 \\ 0 & 0 & A_{45} & A_{55} & 0 & 0 & 0 & 0 \\ A_{16} & A_{26} & 0 & 0 & A_{66} & B_{16} & B_{26} & B_{66} \\ B_{11} & B_{12} & 0 & 0 & B_{16} & D_{11} & D_{12} & D_{16} \\ B_{12} & B_{22} & 0 & 0 & B_{26} & D_{12} & D_{22} & D_{26} \\ B_{16} & B_{26} & 0 & 0 & B_{66} & D_{16} & D_{26} & D_{66} \end{bmatrix} \begin{bmatrix} u_{0,x} \\ v_{0,y} \\ w_{,y} + \psi_y \\ w_{,x} + \psi_x \\ u_{0,y} + v_{0,x} \\ \psi_{x,x} \\ \psi_{y,y} \\ \psi_{x,y} + \psi_{y,x} \end{bmatrix} \tag{2}$$

where $N_1, N_2, \ldots, M_6$ are stress resultants; and material components A_{ij}, B_{ij} and D_{ij} are given by

$$(A_{ij}, B_{ij}, D_{ij}) = \int_{-h/2}^{h/2} Q_{ij}^{(m)}(1, z, z^2)\,\mathrm{d}z \quad (i, j = 1, 2, 6) \tag{3a}$$

and

$$A_{ij} = k_\alpha \cdot k_\beta \cdot \bar{A}_{ij}\,, \qquad \bar{A}_{ij} = \int_{-h/2}^{h/2} Q_{ij}^{(m)}\,\mathrm{d}z \quad (i, j = 4, 5;\ \ \alpha = 6 - i,\ \ \beta = 6 - j) \tag{3b}$$

where Q_{ij} are material constants; the superscript m denotes layer number and k_i are shear correction factors which can be evaluated from the exact expressions given by Whitney [14]. The derivation of the equation of motion for the plate is based on the virtual work equation. The introduction of virtual displacements δu_i to the plate under dynamic equilibrium gives the virtual work equation as [15]

$$\frac{1}{2}\delta \int_V (\sigma_{ij}\varepsilon_{ij})\,\mathrm{d}V + \int_V \rho \ddot{u}_i \delta u_i\,\mathrm{d}V - \int_{S_1} p_i \delta u_i\,\mathrm{d}S = 0 \tag{4}$$

where V is the volume, ρ the mass density, $\ddot{u}_i$ the accelerations and p_i surface tractions acting over the area S_1 of the plate; It is noted that if plate damping is included in the above equation, the moduli will be complex in the form $E^R(1 + \mathrm{i}\eta)$, where E^R is the storage modulus and η the material loss factor, in accordance with the principle of linear viscoelasticity. For simplicity, the damping effect is neglected in the derivation of the equation of motion and frequency analysis of the plate. However, the damping of the plate will be considered separately in the following section on damping analysis of composite plate using the modal damping model constructed via an energy concept.

3. Finite element formulation

The virtual work equation of the plate discretized into NE elements can be written as

$$\sum_{k=1}^{\mathrm{NE}} \left\{ \frac{1}{2}\delta \int_{V_e} (\sigma_{ij}\varepsilon_{ij})\,\mathrm{d}V + \int_{V_e} \rho \ddot{u}_i \delta u_i\,\mathrm{d}V - \int_{S_{1e}} p_i \delta u_i\,\mathrm{d}S \right\}_k = 0 \tag{5}$$

where V_e, S_{1e} is the volume and surface of an element, respectively. The midplane displacements (u_0, v_0, w, ψ_x, ψ_y) within an element are given as functions of $5 \times q$ discrete nodal displacements and in matrix form they are expressed as

$$\boldsymbol{u} = \sum_{i=1}^{q} [H_i \boldsymbol{I}]\boldsymbol{\nabla}_{ei} = \boldsymbol{H}\tilde{\boldsymbol{\nabla}}_e \tag{6}$$

where q is the number of nodes of the element; H_i are shape functions; $\boldsymbol{I}$ is a 5×5 unit matrix; $\boldsymbol{H}$ is shape function matrix; $\tilde{\boldsymbol{\nabla}}_e = \{\boldsymbol{\nabla}_{e1}, \boldsymbol{\nabla}_{e2}, \ldots, \boldsymbol{\nabla}_{eq}\}^{\mathrm{t}}$; and the nodal displacements $\boldsymbol{\nabla}_{ei}$ at a node are

$$\boldsymbol{\nabla}_{ei} = \{u_{0i}, v_{0i}, w_i, \psi_{xi}, \psi_{yi}\}^{\mathrm{t}}\,, \quad i = 1, \ldots, q \tag{7}$$

Substituting Eq. (6) into Eq. (5) and using standard finite element approach to add the contributions of all the elements in the domain, the virtual work equation of the plate becomes

$$\delta \mathbf{\nabla}\{\mathbf{K}\mathbf{\nabla} + \mathbf{M}\ddot{\mathbf{\nabla}} - \mathbf{P}\} = 0 \tag{8}$$

where $\mathbf{M}$, $\mathbf{K}$, $\mathbf{\nabla}$ are the generalized mass matrix, stiffness matrix and displacement vector of the plate, respectively. Since $\delta\mathbf{\nabla}$ is arbitrary, the equation of motion of the plate can be obtained from Eq. (8) as

$$\mathbf{K}\mathbf{\nabla} + \mathbf{M}\ddot{\mathbf{\nabla}} - \mathbf{P} = 0 \tag{9}$$

In the finite element model, a quadratic ($q = 8$) element of the serendipity family with reduced integration of the 2×2 Gauss rule is used. The eigenvalue problem of the plate is expressed in matrix form as

$$\mathbf{K}\mathbf{\nabla} - \omega^2 \mathbf{M}\mathbf{\nabla} = 0 \tag{10}$$

where ω is vibration frequency. It is worthy to note that if the complex moduli in the form $E^R(1 + i\eta)$ are adopted in deriving the above eigenvalue problem, the frequency parameter ω will be complex. The real part, ω_r, of the complex frequency parameter is the resonant frequency, and the ratio of the imaginary part to the real part is the associated system loss factor η_s [4]. When the mode shape vector of the plate has been solved from Eq. (10), the modal maximum strain energy U stored in the plate is computed as

$$U = \frac{1}{2} \mathbf{\nabla}^t \mathbf{K} \mathbf{\nabla} \tag{11}$$

The rates of change of modal strain energy with respect to ply orientations or layer group thicknesses are

$$\frac{\partial U}{\partial X_i} = \frac{1}{2}\left[\left(\frac{\partial \mathbf{\nabla}}{\partial X_i}\right)^t \mathbf{K}\mathbf{\nabla} + \mathbf{\nabla}\mathbf{K}\left(\frac{\partial \mathbf{\nabla}}{\partial X_i}\right) + \mathbf{\nabla}^t\left(\frac{\partial \mathbf{K}}{\partial X_i}\right)\mathbf{\nabla}\right] \tag{12}$$

where X_i may be ply orientations or thicknesses of layer groups.

4. Damping of composite plate

The model used for describing the modal structural damping of a laminated composite plate is based on an energy concept. It can be shown that the modal loss factor η_s of a structure is the ratio of energy dissipated per cycle to the maximum strain energy during the cycle [8].

$$\eta_s = \frac{\Delta U}{U} \tag{13}$$

where ΔU is the energy dissipated during a stress cycle.

If η_1, η_2 are the loss factors of beam specimens with fiber angles 0° and 90°, respectively, which are tested in flexure and η_{12}, η_{23}, η_{13} are the loss factors of 0° and 90° specimens in longitudinal or transverse shear, then by observing the definition of Eq. (13), the total energy dissipated per cycle in the plate can be evaluated from the following expression,

$$\Delta U = \frac{1}{2} \sum_{i=1}^{\mathrm{NE}} \left[\int\!\!\int_{S_e} \int_{-h/2}^{h/2} \boldsymbol{\varepsilon}^{(m)t} \boldsymbol{\eta}^{(m)} \boldsymbol{\sigma}^{(m)} \, \mathrm{d}Z \, \mathrm{d}S \right]_i \tag{14}$$

where $\boldsymbol{\eta}^{(m)}$ is a diagonal matrix containing the material loss factors of the mth ply, or

$$\boldsymbol{\eta} = \begin{bmatrix} \eta_1 & & & & \\ & \eta_2 & & 0 & \\ & & \eta_{23} & & \\ & 0 & & \eta_{13} & \\ & & & & \eta_{12} \end{bmatrix} \tag{15}$$

Observing the constitutive relations and the transformation of quantities between the reference coordinate system and the fiber direction system, Eq. (14) can be written as

$$\Delta U = \sum_{i=1}^{\mathrm{NE}} \left[\frac{1}{2} \int_{S_e} \int_{-h/2}^{h/2} [\bar{\varepsilon}^t T^t \eta Q T \bar{\varepsilon}]^{(m)} \, \mathrm{d}Z \, \mathrm{d}S \right]_i \tag{16}$$

where $\bar{\varepsilon}$ is a vector of strains referred to the reference coordinate system, and T a coordinate transformation matrix. Expressions for evaluating the terms in matrix T can be found in [16]. Let

$$R^{(m)} = [T^t \eta Q T]^{(m)} \tag{17}$$

then Eq. (16) becomes

$$\Delta U = \sum_{i=1}^{\mathrm{NE}} \left[\frac{1}{2} \int_{S_e} \int_{-h/2}^{h/2} [\bar{\varepsilon}^t R \bar{\varepsilon}]^{(m)} \, \mathrm{d}Z \, \mathrm{d}S \right]_i \tag{18}$$

With a similar technique to that used in the finite element method, strains at any point in an element can be evaluated from the nodal displacements as

$$\bar{\varepsilon} = L \tilde{\nabla}_e \tag{19}$$

where L is a matrix of the derivatives of the shape functions. Substitution of Eq. (19) into Eq. (18) gives

$$\Delta U = \sum_{i=1}^{\mathrm{NE}} \frac{1}{2} \tilde{\nabla}_{ei}^t \hat{K}_i \tilde{\nabla}_{ei} \tag{20}$$

and the element damped stiffness matrix

$$\hat{K} = \int_{S_e} \int_{-h/2}^{h/2} [L^t R L]^{(m)} \, \mathrm{d}Z \, \mathrm{d}S \tag{21}$$

In view of the condition of compatibility, the dissipated energy of Eq. (20) can be expressed in terms of the assembled global damped stiffness matrix, K_d, and the global nodal displacements, ∇, as

$$\Delta U = \frac{1}{2} \nabla^t K_d \nabla \tag{22}$$

The rates of change of the dissipated energy with respect to fiber angles or layer group thicknesses can be obtained in a form similar to that of Eq. (12). In view of Eq. (13), the rates of change of the loss factor with respect to design variables are written as

$$\frac{\partial \eta_s}{\partial X_i} = \left[\left(\frac{\partial \Delta U}{\partial X_i} \right) U - \left(\frac{\partial U}{\partial X_i} \right) \Delta U \right] \Big/ (U^2) \tag{23}$$

The above expression will be used in the following optimal design of laminated plates for maximum damping.

5. Optimal layup design

The objective in the present optimal design of a laminated composite plate with given thickness h and number of layer groups NL is the selection of the fiber angles and thicknesses of layer groups which gives the maximum fundamental frequency or modal damping capacity of the plate. In mathematical form, the optimal design problem is stated as

$$\begin{aligned} &\text{Minimize} \quad \Phi(\boldsymbol{\theta}, \boldsymbol{h}) = -q_1 \frac{\eta_s}{\eta_0} - q_2 \frac{\omega_1}{\omega_0} \\ &\text{Subject to} \quad 0^\circ \leq \theta_i \leq 180^\circ \\ &\qquad \sum_{i=1}^{\mathrm{NL}} h_i = h \\ &\qquad h_i \geq 0 \quad i = 1, \ldots, \mathrm{NL} \end{aligned} \tag{24}$$

where q_1, q_2 are weighting factors; $\boldsymbol{h} = (h_1, h_2, \ldots, h_{\mathrm{NL}})^{\mathrm{t}}$, $\boldsymbol{\theta} = (\theta_1, \theta_2, \ldots, \theta_{\mathrm{NL}})^{\mathrm{t}}$ the vectors of layer group thicknesses and fiber angles, respectively; ω_1, η_s, are natural frequency and loss factor (modal damping) of the fundamental vibration mode of the plate; and η_0, ω_0 are some reference values of η_s and ω_1, respectively.

Before proceeding to the solution of the above problem, first consider the special case in which the thicknesses of layer groups have been destined to, say, $h_i = h/\mathrm{NL}$ ($i = 1, \ldots, \mathrm{NL}$) and only fiber angles $\boldsymbol{\theta}$ are treated as design variables. In this case, the optimization problem can be easily solved by the previously proposed unconstrained multi-start global optimization algorithm [9]. The basic idea of the unconstrained multi-start global optimization method is to solve the problem of unconstrained minimization of a differentiable objective function $F(x)$, $x \in X \subset R^n$ and $F \subset C^1$, with several local minima $\hat{F}_j$ and corresponding local minimizers $\hat{x}_j$. It is noted that, for example, in the optimal design of laminated composite plates, $\boldsymbol{x}$ and $F(\boldsymbol{x})$ become $\boldsymbol{\theta}$ and $\boldsymbol{\Phi}(\boldsymbol{\theta})$, respectively. In the global minimization process, a series of starting points are selected at random from the region of interest and a local minimization algorithm is used from each starting point. The search trajectories used by the local minimization algorithm are derived from the equation of motion of a particle of unit mass in an n-dimensional conservative force field, where the potential energy of the particle is represented by $F(\boldsymbol{x}(t))$. In such a field the total energy of the particle, consisting of its potential and kinetic energies, is conserved. The motion of the particle is simulated and by monitoring its kinetic energy an interfering strategy is adopted which ensures that potential energy is systematically reduced. In this way the particle is forced to follow a trajectory towards a local minimum in potential energy, $\hat{\boldsymbol{x}}$. By uninterrupting the motion of the particle with conserved total energy, other lower local minima including in particular the global minimum are obtained and recorded when the particle is traveling along its path. The motion of the particle is stopped once a termination criterion is satisfied. The same procedure is applied to the other starting points. As the process of searching for the global minimum continues, a Bayesian argument [17] is used to establish the probability of the current overall minimum value of F being the global minimum, given the number of starts and number of times this value has been achieved. The multi-start procedure is terminated once a target probability, typically 0.998, has been exceeded. The main advantage of this multi-start global optimization algorithm is that it can determine the global optimal solution in a very efficient and effective way.

Now consider the solution of the optimization problem stated in Eq. (24) in which both fiber angles and thicknesses of layer groups are treated as design variables. Due to the presence of the constraints on layer group and plate thicknesses, the direct application of the unconstrained multi-start global optimization algorithm becomes futile. The constrained optimization problem, however, can be converted to an unconstrained one by creating the general augmented Lagrangian [18]

$$\Psi(\boldsymbol{\theta}, \boldsymbol{h}, \boldsymbol{\lambda}, r_p) = \Phi(\boldsymbol{\theta}, \boldsymbol{h}) + \sum_{j=1}^{\mathrm{NL}} \left[\lambda_j x_j + r_p x_j^2\right] + \left[\lambda_{\mathrm{NL}+1} H + r_p H^2\right] \tag{25}$$

with

$$\begin{aligned} &x_j = \max\left[g_j(h_j), \frac{-\lambda_j}{2r_p} \right] \\ &g_j(h_j) = -h_j \leq 0 \quad j = 1, \ldots, \mathrm{NL} \\ &H = \sum_{i=1}^{\mathrm{NL}} h_i - h = 0 \end{aligned} \tag{26}$$

where λ_j, r_p are multipliers.

The update formulas for the multipliers λ_j and r_p are

$$\begin{aligned}
&\lambda_j^{n+1} = \lambda_j^n + 2r_p^n x_j^n \quad j = 1, \ldots, \mathrm{NL} \\
&\lambda_{\mathrm{NL}+1}^{n+1} = \lambda_{\mathrm{NL}+1}^n + 2r_p^n H^n \\
&r_p^{n+1} = \begin{cases} \gamma r_p^n & \text{if } r_p^{n+1} < r_p^{\max} \\ r_p^{\max} & \text{if } r_p^{n+1} \geq r_p^{\max} \end{cases}
\end{aligned} \tag{27}$$

where the superscript n denotes iteration number, γ is a constant; $r_p^{\max}$ is the maximum value of r_p. The initial values of the multipliers and the values of the parameters (γ, $r_p^{\max}$) are chosen as

$$\begin{aligned}
&\lambda_j^0 = 1.0 \quad j = 1, \ldots, \mathrm{NL} + 1 \\
&r_p^0 = 0.4 \\
&\gamma = 1.25 \\
&r_p^{\max} = 100
\end{aligned} \tag{28}$$

The previously proposed unconstrained multi-start global optimization technique can then be used to solve the problem of Eq. (25). It is noted that in case of optimal design of laminated composite plates for maximum frequency the search direction tends to be controlled by the rates of change of Ψ with respect to layer group thicknesses which may lead to the repeated violation of the constraints and thus the difficulty in convergence of the solution. To circumvent this difficulty, the search direction is determined using the modified gradient of the general augmented Lagrangian in which the components are obtained as

$$\frac{\partial \tilde{\Psi}}{\partial h_i} = \frac{\dfrac{\partial \Psi}{\partial h_i}}{\left[\sum_{i=1}^{\mathrm{NL}} \left(\dfrac{\partial \Psi}{\partial h_i}\right)^2\right]^{1/2}} \tag{29}$$

and

$$\frac{\partial \tilde{\Psi}}{\partial \theta_i} = \frac{\dfrac{\partial \Psi}{\partial \theta_i}}{\left[\sum_{i=1}^{\mathrm{NL}} \left(\dfrac{\partial \Psi}{\partial \theta_i}\right)^2\right]^{1/2}} \quad i = 1, \ldots, \mathrm{NL}$$

Hence, when using the above modified gradient of the general augmented Lagrangian in the optimal design for the maximum frequency, the convergence of the solution can be ensured as will be demonstrated in the following section.

6. Numerical examples

The forementioned global optimization technique will be applied to the design of simply supported rectangular symmetrically laminated composite plates. Before performing the optimal design, it is worth studying the accuracy of the present finite element model in predicting frequency and damping of laminated composite plates. The material properties and dimensions of the square laminated plates used in the verification are listed in Table 1. The plates were analyzed by using a uniform mesh of 4 × 4 quadratic elements. The results obtained by the present method are given in Table 2 in comparisons with the experimental data and finite element results reported in [3]. It is noted that the present finite element model can yield very good results.

Now consider the optimal design of simply supported symmetrically laminated composite plates in which either fiber angles (layer group thicknesses are set to be $h_i = h/\mathrm{NL}$) or both fiber angles and

Table 1
Material properties and plate dimensions used for model verification

Material	E_1 (Gpa)	E_2 (Gpa)	G_{12}, G_{13} (Gpa)	G_{23} (Gpa)	η_1 (%)	η_2 (%)	η_{12} (%)	ν_1, ν_2
CFRP	172.7	7.2	3.76	1.88	0.45	4.22	7.05	0.3
GFRP	37.78	10.9	4.91	2.45	0.87	5.05	6.91	0.3

Plate No.	Material	No. of layers	Density (kg/m³)	Thickness (mm)	Length (mm)	Ply orientation
762	CFRP	8	1566	1.58	178	All 0°
764	CFRP	8	1446	2.12	234	[0°/90°/0°/90°]s
761	GFRP	8	1971	1.64	183	All 0°
734	GFRP	8	1814	2.05	227	[0°/90°/0°/90°]s

Table 2
Comparison of values of natural frequency and damping obtained by different methods

Plate No.	Material	Mode	Adams et al. [3]				Present	
			Experiment		Finite Element		ω_1 (Hz)	η_s (%)
			ω_1 (Hz)	η_s (%)	ω_1 (Hz)	η_s (%)		
762	CFRP	I	81.5	7.0	83.6	6.76	82.2	6.89
762	CFRP	II	107.4	4.9	118.4	4.28	115.2	4.25
764	CFRP	I	68.9	6.7	58.1	7.80	67.8	6.94
761	GFRP	I	78.1	6.0	88.1	5.99	82.2	6.03
734	GFRP	I	62.2	6.7	66.4	7.16	69.7	6.68

thicknesses of layer groups are treated as design variables. The plates are made of glass fiber reinforced plastic (GFRP) with material properties given in Table 1 and the assumption that $\eta_{12} = \eta_{13} = \eta_{23}$. The plates are designed for either maximum fundamental frequency or maximum loss factor of the first mode. In case of maximum frequency design, the weighting factors in Eq. (24) are set as $q_1 = 1$ and $q_2 = 0$. The global optimal solutions for the laminated plates with various aspect ratios, length-to-thickness ratios and numbers of layer groups using either fiber angles or both fiber angles and layer group thicknesses as design variables are given in Tables 3–8 for comparisons. It is noted that higher frequency for plates with $a/b = 1.0$ and 1.5 can be obtained when both layer group thicknesses and fiber angles are treated as design variables. On the other hand, the number of layer groups has some effects on magnitude of frequency for the cases where only fiber angles are treated as design variables and

Table 3
Optimal layups for symmetrically laminated GFRP plates with maximum normalized frequency $\bar{\omega}_1 = \omega_1 b^2\sqrt{\rho/E_2h^2}/(a/b = 1.0, a/h = 10)$

No. of layer groups	Unconstrained optimization [$h_i = h/\mathrm{NL}$]		Constrained optimization		
	Fiber angles (degree)	$\bar{\omega}_1$ / (η_s)[a]	Fiber angles (degree)	Normalized layer thicknesses ($\bar{h}_i = h_i/h$)	$\bar{\omega}_1$ / (η_s)[a]
4	[45/ − 45]s	7.82 (0.0273)	[45/ − 45]s	[0.0968/0.4032]s	8.11 (0.0243)
6	[45/ − 45/45]s	7.98 (0.0251)	[45/ − 45/45]s	[0.0001/0.0967/0.4032]s	8.11 (0.0243)
8	[45/ − 45/45/ − 45]s	8.00 (0.0247)	[45/ − 45/45/ − 45]s	[0.02149/0.05745/0.00002/0.42104]s	8.11 (0.0243)

[a] Modal loss factor associated with maximum frequency.

Table 4
Optimal layups for symmetrically laminated GFRP plates with maximum normalized frequency $\bar{\omega}_1 = \omega_1 b^2\sqrt{\rho/E_2 h^2}$ ($a/b = 1.5$, $a/h = 10$)

No. of layer groups	Unconstrained optimization $[h_i = h/NL]$		Constrained optimization		
	Fiber angles (degree)	$\frac{\bar{\omega}_1}{(\eta_1)^a}$	Fiber angles (degree)	Normalized layer thicknesses ($\bar{h}_i = h_i/h$)	$\frac{\bar{\omega}_1}{(\eta_1)^a}$
4	[90/90]s	$\frac{5.68}{(0.03)}$	[−67.5/69.7]s	[0.0921/0.4079]s	$\frac{5.77}{(0.0269)}$
6	[79/−65/88]s	$\frac{5.7}{(0.028)}$	[−68/66.8/−70]s	[0.0021/0.0939/0.4040]s	$\frac{5.77}{(0.0269)}$
8	[70/−65/−70/83]s	$\frac{5.72}{(0.028)}$	[70/−65/70.2/−83]s	[0.04/0.046/0.037/0.377]s	$\frac{5.77}{(0.0269)}$

[a] Modal loss factor associated with maximum frequency.

Table 5
Optimal layups for symmetrically laminated GFRP plates with maximum normalized frequency $\bar{\omega}_1 = \omega_1 b^2\sqrt{\rho/E_2 h^2}$ ($a/b = 2.0$, $a/h = 10$)

No. of layer groups	Unconstrained optimization $[h_i = h/NL]$		Constrained optimization		
	Fiber angles (degree)	$\frac{\bar{\omega}_1}{(\eta_1)^a}$	Fiber angles (degree)	Normalized layer thicknesses ($\bar{h}_i = h_i/h$)	$\frac{\bar{\omega}_1}{(\eta_1)^a}$
4	[90/90]s	$\frac{5.10}{(0.03)}$	[90/90]s	[0.25/0.25]s	$\frac{5.10}{(0.03)}$
6	[90/90/90]s	$\frac{5.10}{(0.03)}$	[90/90/90]s	[0.16667/0.16667/0.16667]s	$\frac{5.10}{(0.03)}$
8	[90/90/90/90]s	$\frac{5.10}{(0.03)}$	[90/90/90/90]s	[0.125/0.125/0.125/0.125]s	$\frac{5.10}{(0.03)}$

[a] Modal loss factor associated with maximum frequency.

Table 6
Optimal layups for symmetrically laminated GFRP plates with maximum normalized frequency $\bar{\omega}_1 = \omega_1 b^2\sqrt{\rho/E_2 h^2}$ ($a/b = 1.0$, $a/h = 30$)

No. of layer groups	Unconstrained optimization $[h_i = h/NL]$		Constrained optimization		
	Fiber angles (degree)	$\frac{\bar{\omega}_1}{(\eta_1)^a}$	Fiber angles (degree)	Normalized layer thicknesses ($\bar{h}_i = h_i/h$)	$\frac{\bar{\omega}_1}{(\eta_1)^a}$
4	[45/−45]s	$\frac{8.33}{(0.022)}$	[45/−45]s	[0.1018/0.3982]s	$\frac{8.58}{(0.0188)}$
6	[45/−45/45]s	$\frac{8.49}{(0.02)}$	[45/−45/45]s	[0.0472/0.1538/0.299]s	$\frac{8.58}{(0.0188)}$
8	[45/−45/45/−45]s	$\frac{8.56}{(0.019)}$	[45/−45/45/−45]s	[0.0275/0.0643/0.0007/0.407[illegible]]s	$\frac{8.58}{(0.0188)}$

[a] Modal loss factor associated with maximum frequency.

Table 7
Optimal layups for symmetrically laminated GFRP plates with maximum normalized frequency $\bar{\omega}_1 = \omega_1 b^2\sqrt{\rho/E_2 h^2}$ ($a/b = 1.5$, $a/h = 30$)

No. of layer groups	Unconstrained optimization [$h_i = h/\mathrm{NL}$]		Constrained optimization		
	Fiber angles (degree)	$\frac{\bar{\omega}_1}{(\eta_1)^a}$	Fiber angles (degree)	Normalized layer thicknesses ($\bar{h}_i = h_i/h$)	$\frac{\bar{\omega}_1}{(\eta_1)^a}$
4	[84/−66]s	$\frac{6.20}{(0.022)}$	[−65.3/64.7]s	[0.1/0.4]s	$\frac{6.27}{(0.0202)}$
6	[−74/65/71]s	$\frac{6.23}{(0.021)}$	[65.1/−64.2/−74.2]s	[0.0975/0.1834/0.2191]s	$\frac{6.27}{(0.0202)}$
8	[68/−64/−67/−66]s	$\frac{6.25}{(0.021)}$	[68/−64.1/−67/−65.8]s	[0.04528/0.9041/0.36430/0.00001]s	$\frac{6.27}{(0.0202)}$

[a] Modal loss factor associated with maximum frequency.

$a/b = 1.0$ and 1.5. But for the cases where both fiber angles and thicknesses of layer groups are treated as design variables, the number of layer groups has no effect on frequency and the choice of only four layer groups can yield the maximum frequency. The optimal fiber angles change from ±45° to 90° when a/b changes from 1.0 to 2.0 for all the cases considered. Furthermore, the transverse shear deformation also has effects to some extent on the optimal lamination arrangement of the plates. For examples, although fiber angles are the same, the normalized layer group thicknesses of the plates of $a/b = 1.0$ with various number of layer groups are different for different length-to-thickness ratios as shown in Tables 3 and 6; and also for plates of $a/b = 1.5$, both fiber angles and layer group thicknesses are different for different length-to-thickness ratios as shown in Tables 4 and 7.

Next, consider the optimal design of laminated GFRP plates for maximum damping. The weighting factors in Eq. (24) are then set as $q_1 = 0$ and $q_2 = 1$. The global optimal solutions for the plates with various aspect ratios, length-to-thickness ratios, and numbers of layer groups using either fiber angles or both fiber angles and layer group thicknesses as design variables are given in Tables 9–14. It is noted that higher loss factor can be obtained, especially for the plates of $a/b = 1.0$, when both fiber angles and layer group thicknesses are treated as design variables. Other interesting points worth pointing out are: The number of layer groups has no effect on the optimal modal loss factors of the plates under

Table 8
Optimal layups for symmetrically laminated GFRP plates with maximum normalized frequency $\bar{\omega}_1 = \omega_1 b^2\sqrt{\rho/E_2 h^2}$ ($a/b = 2.0$, $a/h = 30$)

No. of layer groups	Unconstrained optimization [$h_i = h/\mathrm{NL}$]		Constrained optimization		
	Fiber angles (degree)	$\frac{\bar{\omega}_1}{(\eta_1)^a}$	Fiber angles (degree)	Normalized layer thicknesses ($\bar{h}_i = h_i/h$)	$\frac{\bar{\omega}_1}{(\eta_1)^a}$
4	[90/90]s	$\frac{5.75}{(0.019)}$	[90/90]s	[0.25/0.25]s	$\frac{5.75}{(0.019)}$
6	[90/90/90]s	$\frac{5.75}{(0.019)}$	[90/90/90]s	[0.16667/0.16667/0.16667]s	$\frac{5.75}{(0.019)}$
8	[90/90/90/90]s	$\frac{5.75}{(0.019)}$	[90/90/90/90]s	[0.125/0.125/0.125/0.125]s	$\frac{5.75}{(0.019)}$

[a] Modal loss factor associated with maximum frequency.

Table 9
Optimal layups for symmetrically laminated GFRP plates with maximum loss factor of the first mode ($a/b = 1.0$, $a/h = 10$)

No. of layer groups	Unconstrained optimization $[h_i = h/NL]$		Constrained optimization		
	Fiber angles (degree)	$\frac{\eta_s}{(\bar{\omega}_1)^a}$	Fiber angles (degree)	Normalized layer thicknesses ($\bar{h}_i = h_i/h$)	$\frac{\eta_s}{(\bar{\omega}_1)^a}$
4	[0/90]s	$\frac{0.0369}{(7.054)}$	[0/90]s	[0.38/0.12]s	$\frac{0.0378}{(7.02)}$
6	[0/0/90]s	$\frac{0.0370}{(7.057)}$	[0/0/90]s	[0.002/0.378/0.12]s	$\frac{0.0378}{(7.02)}$
8	[0/0/0/90]s	$\frac{0.0370}{(7.057)}$	[0/0/0/90]s	[0.0033/0.00070.3760/0.120]s	$\frac{0.0378}{(7.02)}$

[a] Associated normalized frequency $\bar{\omega} = \omega_1 b^2\sqrt{\rho/E_2h^2}$.

Table 10
Optimal layups for symmetrically laminated GFRP plates with maximum loss factor of the first mode ($a/b = 1.5$, $a/h = 10$)

No. of layer groups	Unconstrained optimization $[h_i = h/NL]$		Constrained optimization		
	Fiber angles (degree)	$\frac{\eta_s}{(\bar{\omega}_1)^a}$	Fiber angles (degree)	Normalized layer thicknesses ($\bar{h}_i = h_i/h$)	$\frac{\eta_s}{(\bar{\omega}_1)^a}$
4	[0/0]s	$\frac{0.0463}{(4.414)}$	[0/90]s	[0.4360/0.0640]s	$\frac{0.0475}{(4.39)}$
6	[0/0/0]s	$\frac{0.0463}{(4.414)}$	[0/0/90]s	[0.006/0.430/0.064]s	$\frac{0.0475}{(4.39)}$
8	[0/0/0/0]s	$\frac{0.0463}{(4.414)}$	[0/0/0/90]s	[0.0021/0.0041/0.4302/0.064]s	$\frac{0.0475}{(4.39)}$

[a] Associated normalized frequency $\bar{\omega} = \omega_1 b^2\sqrt{\rho/E_2h^2}$.

Table 11
Optimal layups for symmetrically laminated GFRP plates with maximum loss factor of the first mode ($a/b = 2.0$, $a/h = 10$)

No. of layer groups	Unconstrained optimization $[h_i = h/NL]$		Constrained optimization		
	Fiber angles (degree)	$\frac{\eta_s}{(\bar{\omega}_1)^a}$	Fiber angles (degree)	Normalized layer thicknesses ($\bar{h}_i = h_i/h$)	$\frac{\eta_s}{(\bar{\omega}_1)^a}$
4	[0/0]s	$\frac{0.0516}{(3.468)}$	[0/90]s	[0.455/0.045]s	$\frac{0.052}{(3.49)}$
6	[0/0/0]s	$\frac{0.0516}{(3.468)}$	[0/0/90]s	[0.0001/0.4549/0.045]s	$\frac{0.052}{(3.49)}$
8	[0/0/0/0]s	$\frac{0.0516}{(3.468)}$	[0/0/0/90]s	[0.4005/0.00010.0544/0.045]s/	$\frac{0.052}{(3.49)}$

[a] Associated normalized frequency $\bar{\omega} = \omega_1 b^2\sqrt{\rho/E_2h^2}$.

Table 12
Optimal layups for symmetrically laminated GFRP plates with maximum loss factor of the first mode ($a/b = 1.0$, $a/h = 30$)

No. of layer groups	Unconstrained optimization [$h_i = h/\mathrm{NL}$]		Constrained optimization		
	Fiber angles (degree)	$\frac{\eta_s}{(\bar{\omega}_1)^a}$	Fiber angles (degree)	Normalized layer thicknesses ($\bar{h}_i = h_i/h$)	$\frac{\eta_s}{(\bar{\omega}_1)^a}$
4	[0/90]s	0.0328 (7.488)	[0/90]s	[0.408/0.092]s	0.0329 (7.48)
6	[0/0/90]s	0.0328 (7.488)	[0/0/90]s	[0.399/0.009/0.92]s	0.0329 (7.48)
8	[0/0/0/90]s	0.0328 (7.488)	[0/0/0/90]s	[0.367/0.0020.039/0.092]s/	0.0329 (7.48)

[a] Associated normalized frequency $\bar{\omega} = \omega_1 b^2\sqrt{\rho/E_2h^2}$.

Table 13
Optimal layups for symmetrically laminated GFRP plates with maximum loss factor of the first mode ($a/b = 1.5$, $a/h = 30$)

No. of layer groups	Unconstrained optimization [$h_i = h/\mathrm{NL}$]		Constrained optimization		
	Fiber angles (degree)	$\frac{\eta_s}{(\bar{\omega}_1)^a}$	Fiber angles (degree)	Normalized layer thicknesses ($\bar{h}_i = h_i/h$)	$\frac{\eta_s}{(\bar{\omega}_1)^a}$
4	[0/0]s	0.0437 (4.738)	[0/90]s	[0.463/0.0370]s	0.0439 (4.73)
6	[0/0/0]s	0.0437 (4.738)	[0/0/90]s	[0.2196/0.2434/0.0370]s	0.0439 (4.73)
8	[0/0/0/0]s	0.0437 (4.738)	[0/0/0/90]s	[0.2135/0.0049/0.2446/0.037]s	0.0439 (4.73)

[a] Associated normalized frequency $\bar{\omega} = \omega_1 b^2\sqrt{\rho/E_2h^2}$.

Table 14
Optimal layups for symmetrically laminated GFRP plates with maximum loss factor of the first mode ($a/b = 2.0$, $a/h = 30$)

No. of layer groups	Unconstrained optimization [$h_i = h/\mathrm{NL}$]		Constrained optimization		
	Fiber angles (degree)	$\frac{\eta_s}{(\bar{\omega}_1)^a}$	Fiber angles (degree)	Normalized layer thicknesses ($\bar{h}_i = h_i/h$)	$\frac{\eta_s}{(\bar{\omega}_1)^a}$
4	[0/0]s	0.0487 (3.828)	[0/90]s	[0.4788/0.0212]s	0.0488 (3.83)
6	[0/0/0]s	0.0487 (3.828)	[0/0/90]s	[0.2449/0.2319/0.0212]s	0.0488 (3.83)
8	[0/0/0/0]s	0.0487 (3.828)	[0/0/0/90]s	[0.2538/0.0002/0.2250/0.0212]s	0.0488 (3.83)

[a] Associated normalized frequency $\bar{\omega} = \omega_1 b^2\sqrt{\rho/E_2h^2}$.

consideration; and the optimal fiber angles of the plates are 0°, 90° or a combination of the above two angles.

7. Conclusion

Optimal lamination arrangements of moderately thick laminated composite plates designed for either maximum frequency or maximum loss factor of the fundamental mode have been investigated using a shear deformable finite element and a constrained multi-start global optimization technique. The proposed optimal design algorithm appears to yield global optimal fiber angles and layer group thicknesses in a efficient and effective way. Results for simply supported symmetrically laminated GFRP plates of various aspect ratios, length-to-thickness ratios, and numbers of layer groups were obtained and their physical implications discussed. It has been shown that in the present approach the use of fiber angles and layer group thicknesses as design variables can greatly reduce the number of layer groups for achieving optimal dynamic characteristics of laminated plates and thus simplify the design and manufacturing processes.

Acknowledgment

This work was supported by the National Science Council of the Republic of China under Grant No. NSC-83-0401-E-009-103.

References

[1] R.G. Ni and R.D. Adams, The damping and dynamic moduli of symmetric laminated composite beams, theoretical and experimental results, J. Composite Materials 18 (1984) 104–121.
[2] R.D. Adams and D.G.C. Bacon, Effect of fiber orientation and laminated geometry on the dynamic properties of CFRP, J. Composite Materials 7 (1973) 402–428.
[3] D.X. Lin, R.G. Ni and R.D. Adams, Prediction and measurement of the vibrational damping parameters of carbon and glass fiber-reinforced plastic plates, J. Composite Materials 18 (1984) 135–152.
[4] N. Alam and N.T. Asnani, Vibration and damping analysis of fiber reinforced composite material plates, J. Composite Materials 20 (1986) 2–18.
[5] C.I. Wu and J. Vinson, Influences of large amplitudes, transverse shear deformation, and rotary inertia on lateral vibrations of transversely isotropic plates, J. Appl. Mech., Trans. ASME 36 (1969) 254–260.
[6] C.W. Bert, Optimal design of composite material plates to maximize its fundamental frequency, J. Sound Vibration 50 (1977) 229–237.
[7] Y.V.K.S. Rao and B.C. Nakra, Vibration of unsymmetrical sandwich beams and plates with viscoelastic cores, J. Sound Vibration 34 (1974) 309–326.
[8] E.E. Ungar and E.M. Jr. Kerwin, Loss factors of viscoelastic systems in terms of energy concepts, J. Acoust. Soc. Amer. 34 (1962) 954–957.
[9] T.Y. Kam and J.A. Snyman, Optimal design of laminated composite plates using a global optimization technique, J. Composite Structures 19 (1991) 351–370.
[10] T.Y. Kam and R.R. Chang, Optimal layup of thick laminated composite plates for maximum stiffness, J. Engrg. Optim. 19 (1992) 237–249
[11] T.Y. Kam and R.R. Chang, Design of laminated composite plates for maximum buckling load and vibration frequency, Comput. Methods Appl. Mech. Engrg. 106 (1993) 65–81.
[12] R.R. Chang, G.H. Chu and T.Y. Kam, Design of laminated composite plates for maximum shear buckling loads, ASME J. Energy Resources Technology, 115 (1993) 314–322.
[13] T.Y. Kam and R.R. Chang, Finite element analysis of shear deformable laminated composite plates, ASME J. Energy Res. Technol. 115 (1993) 41–46.
[14] J.M. Whitney, Shear correction factors for orthotropic laminates under static load, J. Appl. Mech. 40 (1973) 302–304.
[15] K. Washizu, Variational Methods in Elasticity and Plasticity (Pergamon Press, New York, 1982).
[16] S.W. Tsai and H.T. Hahn, Introduction to composite materials, Technomic, Westport, CT, USA, 1980.

[17] J.A. Snyman and L.P. Fatti, A multi-start global minimization algoritm with dynamic search trajectories, J. Optim. Theory Appl. 54 (1987) 121–141.

[18] G.N. Vanderplaats, Numerical Optimization Techniques for Engineering Design: With Applications (McGraw-Hill, Inc., New York, 1984).